Polymer Vol. 38 No. 15, pp. 3719–3725, 1997

0032-3861/97/$17.00 + 0.00

PII: S0032-3861(96)00952-4

polymer papers

N.m.r. and d.s.c. investigations of the miscibility of poly(methyl methacrylate)/ poly(ethylene oxide) blends

N. Parizel*
Institut Charles Sadron, CNRS–ULP Strasbourg, 6 rue Boussingault, 67083 Strasbourg Cedex, France

and F. Lauprêtre and L. Monnerie
Laboratoire de Physico-Chimie Structurale et Macromoléculaire associé au CNRS, ESPCI, 10 rue Vauquelin, 75231 Paris Cedex 05, France
(Revised 7 October 1996)

^{1}H spin-lattice relaxation times in the rotating frame and free induction decays were measured on poly(methyl methacrylate)/poly(ethylene oxide) blends over the whole composition range. In these systems, in which one component is an amorphous polymer and the other one can crystallize, experiments combining both ^{1}H and ^{13}C n.m.r. spectroscopies allowed the determination of the composition of each phase. Results thus obtained led to the conclusion that phase separation occurs during the freeze-drying step. Therefore, poly(ethylene oxide) crystallization takes place in a poly(ethylene oxide) rich phase. © 1997 Elsevier Science Ltd.

(Keywords: poly(methyl methacrylate)/poly(ethylene oxide) blends; n.m.r.)

INTRODUCTION

In amorphous polymer blends, three different types of behaviour may be encountered; either the polymers are immiscible over the whole composition and temperature ranges, or the polymers are miscible over the whole composition range for the temperatures at which they are stable, or the polymers are partly miscible. In the last situation, thermodynamic equilibrium corresponds either to a single phase or to two phases, each of them being enriched in one of the two components. In contrast, when one blend component is a semicrystalline polymer and crystallization phenomena occur, the bulk organization at the molecular level may be more complex.

Amorphous poly(methyl methacrylate) (PMMA)/ poly(ethylene oxide) (PEO) blends are a typical example of blends containing both an amorphous and a semicrystalline component. PMMA/PEO blends have already been extensively studied by a number of experimental techniques such as differential scanning calorimetry[1–3], rheology[4–9], optical[10–16] and electron[17,18] microscopies, small-angle X-ray scattering[19–22], small angle neutron scattering[23,24], Fourier transform infrared spectroscopy[25–28], electron spin resonance[29,30] and nuclear magnetic resonance[28,31]. Although a few papers indicate that some phase separation in the amorphous phase may occur[3,22], the more frequent conclusions are that the two polymers are miscible in the amorphous phase of the blend. These results are corroborated by determinations of the polymer–polymer interaction parameter, which varies from -5×10^{-3} to -1×10^{-3} as the total PMMA concentration increases from 0.3 to 0.7[23]. However, within the limits of our knowledge, no phase diagram has been established over the whole composition range and the composition of the amorphous phase has not been determined in semicrystalline blends.

Among the methods which permit investigation of the solid-state organization of polymers, ^{1}H n.m.r. is of primary importance. The dependence of free induction decay on mobility and internuclear distances provides a means for quantitatively determining the composition of the different phases. Besides, in an inhomogeneous material, the spin-lattice relaxation times in the rotating and laboratory frames are very sensitive to the size of the domains, which makes them powerful tools for studying miscibility. Moreover, selective information on the specific behaviour of each component in the blend can be obtained by taking advantage of cross-polarization phenomena between proton and carbon 13 nuclei and measuring ^{1}H relaxation data by means of high-resolution solid-state ^{13}C n.m.r.

The present paper is devoted to the investigation of the miscibility and phase composition of poly(methyl methacrylate)/poly(ethylene oxide) blends over their whole composition range by using d.s.c. as well as ^{1}H and high-resolution solid-state ^{13}C n.m.r. determinations of ^{1}H free induction decays and ^{1}H spin-lattice relaxation times in the rotating and laboratory frames.

EXPERIMENTAL

Materials

PMMA was supplied by ICI. It contains a low amount of acrylic comonomer. Its taciticity, as determined by ^{1}H

* To whom correspondence should be addressed

n.m.r., is rr = 53%; rm = 40% and mm = 7%. Its molecular weights, as measured by gel permeation chromatography, are: $M_n = 61\,750$ and $M_w = 117\,000$.

PEO ($M_w = 20\,000$) was supplied by Merck–Schuchardt.

Sample preparation

PEO and PMMA samples were dissolved in benzene at the desired composition. The solution was stirred for 96 h. Freeze-drying was performed on solutions containing 1 g polymer in 20 ml of benzene. The duration of freeze-drying was 24 h. Then, in order to melt the crystalline PEO and to improve the homogenization of the two polymers in the miscible phase, samples were annealed for 24 h at 10 K above the PEO melting temperature or the glass transition temperature of the blend, T_g, when T_g was higher than T_m.

PMMA/PEO blends are referred to herein as (*a*/*b*) (PMMA/PEO) blends, where *a* and *b* are the weight fractions of PMMA and PEO, respectively.

Differential scanning calorimetry

Glass transition temperatures, T_g, were measured using a differential scanning calorimeter (d.s.c.) (DuPont 1090) operating at 10 K min^{-1}. The glass transition temperature was estimated from the intersection of the initial baseline and the sloping portion of the baseline due to the glass transition phenomenon.

The apparent enthalpies of melting and melting temperatures were derived from the area and maxima of the endothermic peaks, respectively. The degrees of crystallinity were calculated from the following equations:

$$\chi_{c\,(PEO)} = \frac{\Delta H^*_{(PEO)}}{\Delta H^0_{(PEO)}}$$

and

$$\chi_{c\,(blend)} = \frac{\Delta H^*_{(blend)}}{\Delta H^0_{(PEO)}}$$

where $\Delta H^0_{(PEO)}$ is the heat of melting per gram of 100% crystalline PEO: $\Delta H^0_{(PEO)} = 205$ J g^{-1} [17]; and where $\Delta H^*_{(PEO)}$ and $\Delta H^*_{(blend)}$ are the apparent enthalpies of melting per gram of PEO and per gram of blend, respectively.

Nuclear magnetic resonance

^{1}H n.m.r. experiments were carried out at 100 MHz with a Bruker CXP 100 spectrometer. ^{1}H free induction decays were measured using the solid-echo pulse sequence[32,33]. The 90° pulse length was taken as 4 μs. The spin-lattice relaxation time in the rotating frame, $T_{1\rho}(^1H)$, was determined by incrementation of the time during which the spin-locking field, of 25 kHz, was applied. The spin-lattice relaxation time, $T_1(^1H)$, was obtained by using the classical inversion–recovery (180°, *t*, 90°) pulse sequence.

High-resolution solid-state ^{13}C n.m.r. experiments using proton dipolar decoupling (DD), magic-angle spinning (MAS) and cross-polarization (CP) were conducted at 75 MHz with a Bruker CXP 300 spectrometer, with quadrature detection and a single r.f. coil, which was double-tuned for both ^{13}C and ^{1}H. Experiments were performed on magic-angle spinning samples contained in Al_2O_3 rotors. The spinning speed was of the order of 4 kHz. The pulse sequence used for the determination of the ^{1}H spin-lattice relaxation times in the rotating frame was the delayed-contact, cross-polarization pulse sequence described in refs 34 and 35. For the $T_2(^1H)$ measurements, the pulse sequence is almost the same but, of course, no spin-lock field is present during the delay before the contact[36]. The matched spin-lock cross-polarization transfers and $T_{1\rho}(^1H)$ determinations were carried out with ^{13}C and ^{1}H magnetic field strengths of 64 kHz. Spin-temperature inversion techniques allowed the minimization of baseline noise and roll[37]. Flip-back[38] was also used to shorten the delay between two successive pulse sequences.

RESULTS AND DISCUSSION

The glass transition temperatures, as determined by d.s.c. for homopolymers and blends containing 80% or more PMMA, are listed in *Table 1* for the various samples. For blends with less than 80% PMMA, the melting peak hides the d.s.c. manifestation of the T_g.

The melting temperatures and crystallinity degrees of blends having more than 40% PEO are reported in Table 2.

Melting–recrystallization cycles were performed on pure PEO and (20/80) and (40/60) (PMMA/PEO) blends. The sample was first heated at 20 K min^{-1} up to 393 K. This last temperature was maintained for 2 min, after which the sample was cooled at 50 K min^{-1}. The crystallization peak was shown to be larger in pure PEO than in the blends. However, whatever the sample, the position of the maximum of the crystallization peak lies in the range between 297 and 303 K, which indicates that the samples can crystallize at room temperature.

From the d.s.c. results, it clearly appears that PEO/PMMA blends belong to two categories, semi-crystalline ones containing more than 20% PEO, and amorphous ones containing at least 80% PMMA. In the following sections, the behaviour of the neat components, the semicrystalline blends and the amorphous blends are examined successively by n.m.r.

Individual blend components

Results of the determinations of spin-lattice relaxation times in the laboratory and in the rotating frame, and of free induction decays, are summarized in *Table 3* for the homopolymers.

Table 1 T_g for blends with 80% or more PMMA and for pure PEO

%PMMA	100	95	90	80	PEO
T_g (K)	378	373	347	320	213

Table 2 Melting temperature and degree of crystallinity for blends having 40% or more PEO

Sample	Melting temperature (K)	Degree of crystallinity (PEO) (%)	Degree of crystallinity (blend) (%)
PEO	339	75	75
PEO 80%	334	72	58
PEO 60%	334	52	31
PEO 50%	334	50	25
PEO 40%	337	28	11

Table 3 Spin-lattice relaxation times in the laboratory and in the rotating frame, and free induction decay decomposition for the individual blend components

	T_1 (s)	$T_{1\rho}$ (ms)	Free induction decay
PMMA	0.27	14.0	Gaussian function $M_2 = 13\,G^2$
PEO	0.08 0.80	0.2 3.0	85% Weibull function ($n = 1.4$) $T_2 = 20\,\mu s$ 13.5% exponential function $T_2 = 38\,\mu s$ 1.5% exponential function $T_2 = 245\,\mu s$

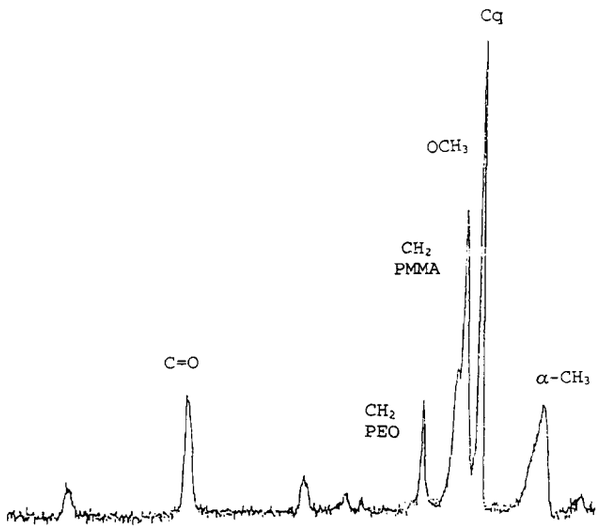

Figure 1 High-resolution solid-state ^{13}C n.m.r. spectrum of the (20/80) (PMMA/PEO) blend

PMMA is characterized by a single $T_1(^1H)$ and a single $T_{1\rho}(^1H)$ at room temperature. Its free induction decay is well described by a gaussian function with a 13 G^2 second moment. These results are consistent with data usually observed on amorphous glassy polymers.

The spin-lattice relaxations of the PEO protons in the rotating and laboratory frames are not exponential. They are well described by a sum of two exponential functions. According to ref. 39, the short spin-lattice relaxation times (0.08 s in the laboratory frame and 0.2 ms in the rotating frame) can be associated with the protons of the crystalline parts of PEO.

The PEO free induction decay exhibits a multi-component behaviour. As indicated in *Table 3*, the short-time behaviour is well represented by a Weibull function. It corresponds to 85% of the protons of the sample and can be assigned to rigid PEO units. The difference between the amount of rigid PEO units and the degree of crystallinity (75 wt% as obtained from d.s.c.) is an indication of the extent (~10%) of the constraint regions of amorphous PEO in the neighbourhood of the crystalline lamellae. The 13.5% PEO having a longer spin–spin relaxation time of 38 μs can be associated with the 'free' amorphous chains. The long-time part of the free induction decay is probably due to a small number of water molecules trapped in the polymer structure.

Semi-crystalline blends

(20/80) (PMMA/PEO) blend. The ^1H spin-lattice relaxation times in the rotating frame, $T_{1\rho}(^1H)$, of the (20/80) (PMMA/PEO) blend at room temperature were determined by high-resolution, solid-state ^{13}C n.m.r. The ^{13}C n.m.r. spectrum of the blend is plotted, and the line assignment summarized, in *Figure 1*. As shown in *Figure 2*, the intensity dependence of the PMMA carbon resonances is an exponential function of the delay time in the delayed-contact, cross-polarization pulse sequence. It is characterized by a (6 ± 1) ms $T_{1\rho}(^1H)$. It is interesting to note that, within the sensitivity of the experiment, the PMMA decay is strictly exponential, which indicates that local PMMA heterogeneities are not detected at the PEO crystallization front, as was

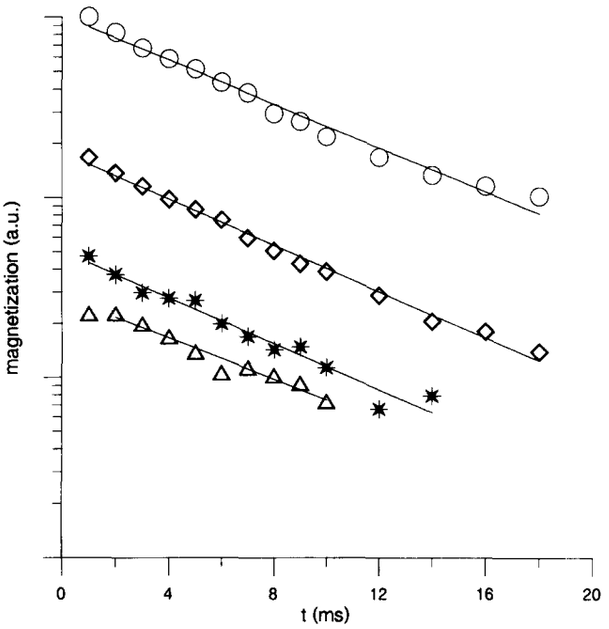

Figure 2 Room temperature $T_{1\rho}(^1H)$ decays obtained in the (20/80) (PMMA/PEO) blend for the PMMA nuclei. ○: C_q; ◇: OCH_3; *: C=O; △: α-CH_3

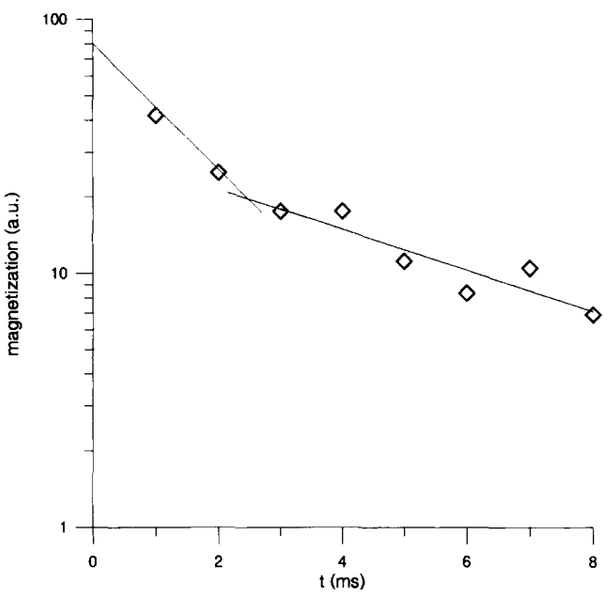

Figure 3 Room temperature $T_{1\rho}(^1H)$ decays obtained in the (20/80) (PMMA/PEO) blend for the PEO nuclei

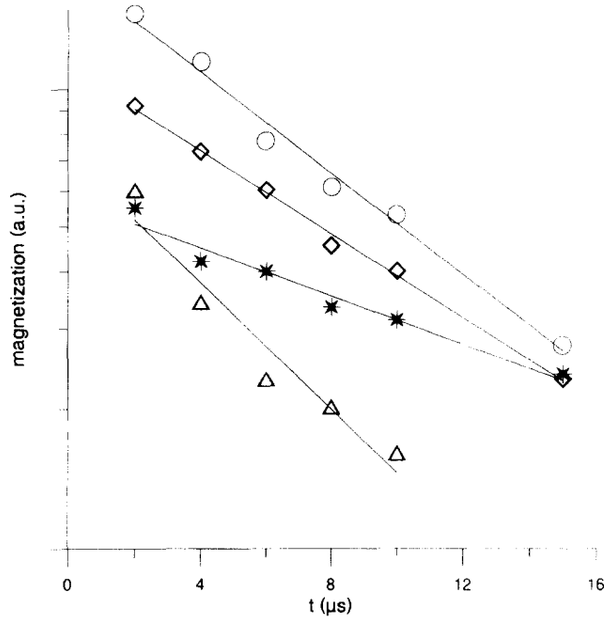

Figure 4 ^{1}H free induction decays determined from high-resolution solid-state ^{13}C n.m.r. at room temperature for the (20/80) (PMMA/PEO) blend. ○: C_q; ◇: OCH_3; △: C=O; *: CH_2 PEO

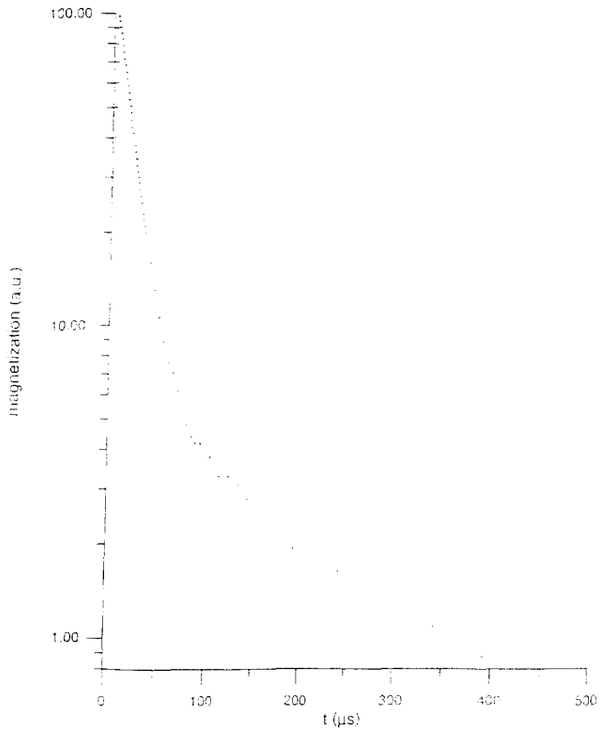

Figure 5 Free induction decays of the (20/80) (PMMA/PEO) blend as determined from ^{1}H n.m.r. at room temperature

observed in blends of PMMA with poly(vinylidene-fluoride)[40].

$T_{1\rho}(^{1}H)$ determination for the PEO nuclei in the blend was performed using the 72 ppm line. As shown in *Figure 3*, the PEO decay is well described by two $T_{1\rho}(^{1}H)$ values of (2 ± 1) ms and (5 ± 1) ms. The $T_{1\rho}(^{1}H)$ values of 6 and 5 ms determined for PMMA and PEO, respectively, can be considered as identical within experimental error. Since these values are intermediate between those of the individual blend components, they are characteristic of polymers in a miscible amorphous phase. It is interesting to estimate the composition of this phase from the relationship proposed by Dickinson[41]. In a miscible blend of two polymers A and B, the $T_{1\rho}(^{1}H)$ of the blend can be written as:

$$\frac{1}{T_{1\rho}(^{1}H)_{AB}} = \left(\frac{N_A}{N}\frac{M_A}{T_{1\rho}(^{1}H)_A}\right) + \left(\frac{N_B}{N}\frac{M_B}{T_{1\rho}(^{1}H)_B}\right)$$

where $T_{1\rho}(^{1}H)_A$ and $T_{1\rho}(^{1}H)_B$ are the relaxation times of the homopolymers A and B, M_A and M_B are the molar fractions of each polymer, and N_A and N_B are the numbers of protons contained in each monomer unit.

Use of this equation for the (20/80) (PMMA/PEO) blend leads to a PMMA content in the miscible phase of the blend of the order of 60 to 80 wt%. It corresponds to a significantly PMMA-enriched phase. This result is, at least partly, due to PEO crystallization, which decreases the amount of PEO available in the miscible amorphous phase.

By comparison with results derived for pure PEO, the $T_{1\rho}(^{1}H)$ value of (2 ± 1) ms observed for PEO can be assigned to constraint PEO chains. It should be noted that crystalline PEO, which has a very short $T_{1\rho}(^{1}H)$, cannot be detected in cross-polarization pulse sequences using a 1 ms contact time.

Free induction decays determined from high-resolution solid-state ^{13}C n.m.r. are shown in *Figure 4*. In the miscible amorphous phase of the blend, the $T_2(^{1}H)$ values of PEO and PMMA are of the order of 20 μs and 10 μs, respectively.

In *Figure 5* is plotted the free induction decay of (20/80) (PMMA/PEO) blend as determined from ^{1}H n.m.r. The fastest decay can be assigned to the sum of three contributions: PMMA protons and PEO protons in the crystalline and constraint units. The intermediate decay is due to PEO in the miscible amorphous phase. The long-time decay is associated with some residual water. Since the amounts of PMMA and crystalline PEO protons are known from the synthesis and degree of crystallinity, respectively, the amount of constraint PEO units can be derived from the magnetization associated with the short-time decay. The amount of PEO units in the miscible amorphous phase is obtained from the magnetization associated with the intermediate decay.

Results thus obtained show that the solid-state organization of the (20/80) (PMMA/PEO) blend can be summarized as follows: a large crystalline phase (57% of the total amount of PEO); constraint PEO units (19% of the total amount of PEO) in the neighbourhood of the crystalline lamellae, characterized by a T_2 smaller than 20 μs and a 2 ms $T_{1\rho}(^{1}H)$; and a miscible amorphous phase which is rich in PMMA (86% from the free induction decay decomposition and between 60 and 80% from the Dickinson equation).

(40/60), (50/50) and (60/40) (PMMA/PEO) blends. The ^{1}H spin-lattice relaxation of the (40/60), (50/50) and (60/40) (PMMA/PEO) blends is not exponential. It is well described by a sum of two exponential functions with $T_1(^{1}H)$ equal to 0.1 s and 0.3–0.4 s, respectively, the exact value depending on the blend composition. The existence of two $T_1(^{1}H)$s, and the fact that the shorter $T_1(^{1}H)$ is close to the crystalline PEO $T_1(^{1}H)$, are evidence that the sizes of the different domains containing PEO units are larger than 100 Å.

Table 4 $T_{1\rho}(^1H)$ values of semi-crystalline blends of PMMA/PEO measured by high resolution solid state ^{13}C n.m.r.

% PMMA	PMMA $T_{1\rho}(^1H)$ (ms)	PEO $T_{1\rho}(^1H)$ (ms)
60	7	7
		2
50	7	7
		2
40	8	8
		2

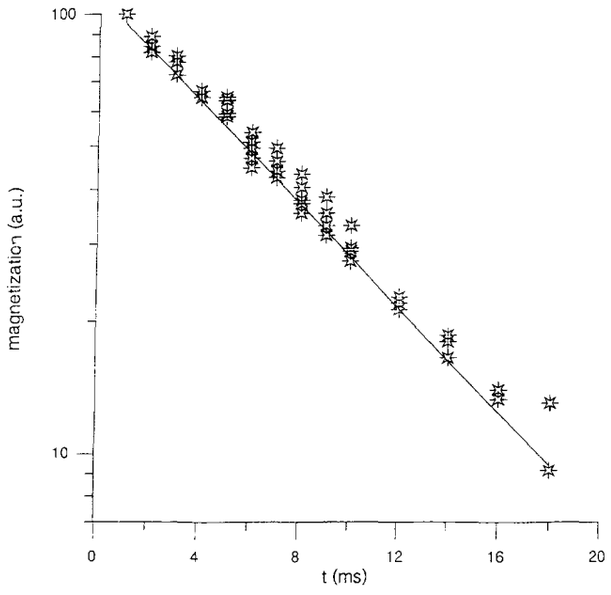

Figure 6 Room temperature $T_{1\rho}(^1H)$ decays obtained in the (60/40) (PMMA/PEO) blend for the PMMA nuclei

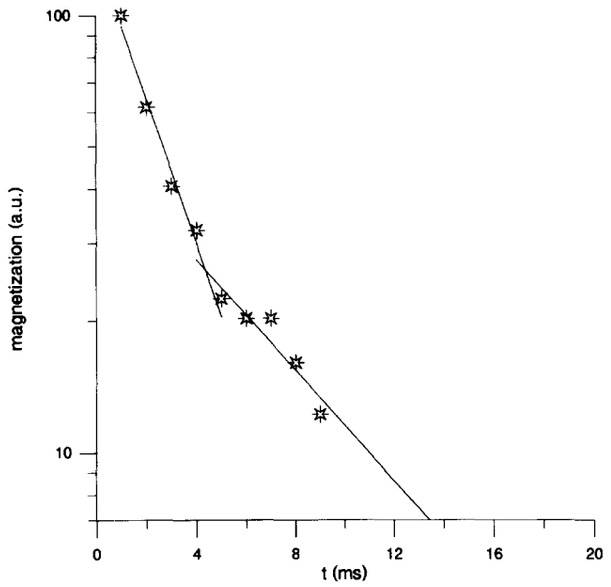

Figure 7 Room temperature $T_{1\rho}(^1H)$ decays obtained in the (60/40) (PMMA/PEO) blend for the PEO nuclei

$T_{1\rho}(^1H)$ decays, determined by ^1H n.m.r. on the (60/40) and (40/60) (PMMA/PEO) blends, are well described by a sum of two exponential functions with $T_{1\rho}(^1H)$ values of (0.5 ± 0.1) ms and (11 ± 1) ms. The faster decay can be assigned to crystalline PEO. It cannot be detected by a 1 ms contact time cross-polarization. The (11 ± 1) ms $T_{1\rho}(^1H)$ lies in the range between the $T_{1\rho}(^1H)$ of the individual blend components. It can therefore be associated with the amorphous PMMA-enriched miscible phase. This assignment is supported by $T_{1\rho}(^1H)$ values determined by using high-resolution solid-state ^{13}C n.m.r. in the different blends and listed in *Table 4*. As an example, the room temperature $T_{1\rho}(^1H)$ decays obtained in the (60/40) (PMMA/PEO) blend for the PMMA and PEO nuclei are shown in *Figures 6* and *7* respectively. For each blend composition, the $T_{1\rho}(^1H)$ decay at long times is identical for the PMMA and the PEO nuclei. This is the signature of an amorphous phase with PMMA and PEO chains mixed at the molecular level. The short-time behaviour of the $T_{1\rho}(^1H)$ decay observed for the PEO nuclei corresponds to the constraint PEO units, as discussed above for the (20/80) (PMMA/PEO) blend.

The analysis of the free induction decay of the blends at room temperature is summarized in *Table 5*. As previously observed, the free induction decay of the PMMA protons is faster than the decay of the PEO protons located in the amorphous phase of the blend. This set of results indicates that the short-time component in the ^1H free induction decay corresponds to both PMMA protons and protons in the crystalline or constraint regions of PEO, whereas the intermediate decay is assigned to PEO protons in the amorphous phase of the blend. The compositions of the different phases of the PMMA/PEO blends were derived from the relative contributions of the intermediate and short-time decays to the free induction decay. Results are given in *Table 6*.

These results clearly demonstrate that, for these semi-crystalline samples, the amorphous phase has a constant composition which is independent of the relative PMMA/PEO contents. It is characterized by a high PMMA content corresponding to a glass transition temperature, T_g, of the order of 343 K. Since such a high PMMA content results in a T_g much higher than the PEO crystallization temperature (~303 K), these observations can be understood only by assuming that, during the cooling of the blend in benzene solution before the freeze-drying, a phase separation happens, which leads to PEO-enriched domains in which PEO crystallization occurs. Simultaneously, a PMMA-enriched phase is created.

To check the occurrence of phase separation during the cooling before the freeze-drying, (50/50) and (70/30) (PMMA/PEO) blends were annealed for 24 h at 343 K. Then they were quenched in liquid nitrogen and examined as obtained or after another 20 h annealing at 318 K. The first set of samples shows the exact features described in the previous sections. However, after the second annealing, the ^{13}C n.m.r. spectrum exhibits a thin high line for the PEO resonance (*Figure 8*). Since the

Table 5 Free induction decay decomposition of semi-crystalline blends

PMMA (wt%)	Fast decay ($M_2 \approx 13\,G^2$) (^1H%)	Intermediate decay ($T_2 \approx 38\,\mu s$) (^1H%)	Slow decay ($T_2 \approx 245\,\mu s$) (^1H%)
60	91.3	7.5	1.2
50	94.1	5	0.9
40	93.1	6	0.9

Table 6 Composition of the different phases of the PMMA/PEO semi-crystalline blend

PMMA/PEO blend % (w/w)	PMMA in the blend % (w/w)	PEO repartition in the blend % (w/w)		Composition of the blended amorphous phase (PMMA/PEO) % (w/w)
		crystalline or constraint phase	blended amorphous phase	
60/40	60	32.8	7.2	89.3/10.7
50/50	50	45.2	4.8	91.2/8.8
40/60	40	54.2	5.8	87.4/12.6

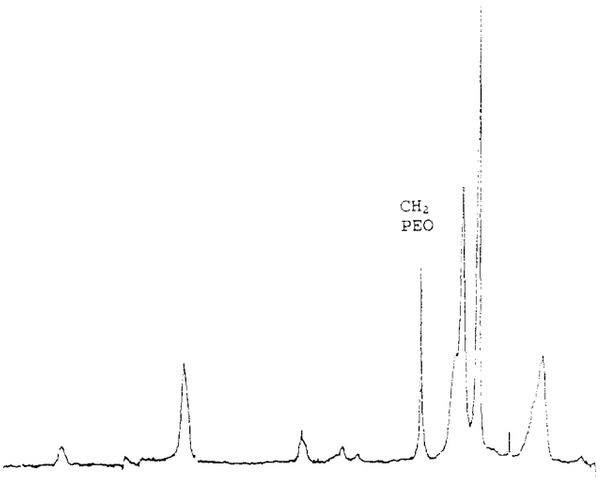

Figure 8 High-resolution solid-state ^{13}C n.m.r. spectrum of a twice annealed (20/80) (PMMA/PEO) blend

Table 7 $T_{1\rho}(^1H)$ for amorphous blends

Blend composition (PMMA/PEO)	$T_{1\rho}(^1H)$ (ms)
(95/5)	11 ± 1
(90/10)	10 ± 0.5
(80/20)	9 ± 1

Table 8 Free induction decay composition of the (80/20) (PMMA/PEO) blend

Rapid decay	Intermediate decay	Slow decay
83% (^1H) gaussian function $M_2 = 13\,G^2$	15% (^1H) exponential 38 μs	2% (^1H) exponential 245 μs

crystalline PEO carbons do not appear in the high resolution spectrum, the intensity of the PEO line indicates that the annealing at 343 K has increased the amount of PEO in the miscible amorphous phase to the detriment of crystalline PEO units. The PEO-rich phase where the PEO crystallizes is not at thermodynamic equilibrium at 343 K, which explains why, on annealing, it gradually disappears in favour of the miscible amorphous phase.

Amorphous blends

The $T_{1\rho}(^1H)$ data of the (95/5), (90/10) and (80/20) (PMMA/PEO) blends are summarized in *Table 7*. For the (95/5) and (90/10) (PMMA/PEO) blends, the composition of the amorphous phase, derived from the Dickinson equation, is identical to the initial blend composition. The same calculation for the (80/20) (PMMA/PEO) blend indicates that the relative amount of PMMA is slightly higher than 80% in the miscible amorphous phase, which implies that some PEO units are not in the miscible phase. This result is consistent with data derived from the analysis of the free induction decay and listed in *Table 8*, which point out the existence of 5 wt% constraint and crystalline PEO. It should be noted that no evidence of a small amount of crystalline PEO is found by d.s.c., probably because it is below the detection threshold of the apparatus.

CONCLUSION

Differential scanning calorimetry results and ^1H and high resolution solid-state ^{13}C nuclear magnetization resonance have led to an accurate description of the bulk organization of PMMA/PEO blends over the whole composition range at room temperature.

For PEO-rich blends, the miscibility, at the molecular level, of the PEO and PMMA chains in the amorphous phase was demonstrated. Although, for some blend compositions, the melting peak of crystalline PEO may hide the manifestation of the glass transition phenomenon, an estimate of the composition of the miscible amorphous phase was derived from the n.m.r. data. Evidence was found for a phase separation that occurs during the cooling of the blend solution before the freeze-drying step. As a result, PEO crystallization takes place in a PEO-rich phase. From this point of view, the (70/30) (PMMA/PEO) sample is an interesting example. From a thermodynamic point of view, it is homogeneous at 343 K. However, when this blend has undergone a phase separation during sample preparation, it has to be annealed for four days at $T_g + 40$ K to be homogeneous at the spatial scale of the n.m.r. experiments. It is also of interest to note that, in highly crystalline blends that have not yet reached thermodynamic equilibrium, local PMMA heterogeneities at the crystallization front were not found. This behaviour, which is opposite to the one observed in blends of PMMA with poly(vinylidene fluoride), results from the fact that, in these PEO-rich blends such as the (20/80) (PMMA/PEO) blend, the glass transition temperature of the blend is below room temperature and, therefore, holding the sample at room temperature is equivalent to an annealing.

For samples that appear amorphous by d.s.c., the miscibility of the two blend components has also been established. In the (95/5) and (90/10) (PMMA/PEO) blends, the composition of the amorphous phase is given by the relative amounts of the two components. However, the (80/20) (PMMA/PEO) sample exhibits an amorphous phase, which is slightly enriched in

PMMA. The small crystalline content of this sample, which was detected by n.m.r., could not be observed by d.s.c.

REFERENCES

1. Liberman, S. A. and Gomes, A. De S., *J. Polym Sci.: Part A: Polym Chem.*, 1984, **22**, 2809.
2. Addonizio, M. L., Martuscelli, E. and Silvestre, C., *Polymer*, 1987, **28**, 183.
3. Zschuppe, V., Unger, R. and Donth, E., *Acta Polymerica*, 1988, **39**, 257.
4. Martuscelli, E., Vicini, L. and Seves, A., *Makromol. Chem., Rapid Commun.*, 1984, **5**, 255.
5. Souheng Wu, *J. Polym. Sci.: Part B: Polym. Phys.*, 1987, **25**, 2511.
6. Calahorra, E., Cortazar, M. and Guzman, G. M., *J. Polym. Sci., Polym. Lett. Ed.*, 1985, **23**, 257.
7. Martuscelli, E., Vicini, L. and Seves, A., *Makromol. Chem.*, 1987, **188**, 607.
8. Runt, J. P., Barron, C. A., Zhang, X. F. and Kumar, S. K., *Macromolecules*, 1991, **24**, 3466.
9. Cardenas-Valera, A. E. and Bailey, A. I., *Colloids and Surfaces, A: Physicochem. and Eng. Aspects*, 1993, **79**, 115.
10. Calahorra, E., Cortazar, M. and Guzman, G. M., *Polymer*, 1982, **23**, 1322.
11. Cortazar, M. M., Calahorra, M. E. and Guzman, G. M., *Eur. Polym. J.*, 1982, **18**, 165.
12. Calahorra, E., Cortazar, M. and Guzman, G. M., *Polymer*, 1982, **23**, 1322.
13. Calahorra, E., Cortazar, M. and Guzman, G. M., *Polym. Commun.*, 1983, **24**, 211.
14. Martuscelli, E., Pracella, M. and Wang Ping Yue, *Polymer*, 1984, **25**, 1097.
15. Alfonso, G. C. and Russell, T. P., *Macromolecules*, 1986, **19**, 1143.
16. Bartczak, Z. and Martuscelli, E., *Makromol. Chem.*, 1987, **188**, 445.
17. Martuscelli, E., Silvestre, C., Addonizio, M. L. and Amelino, L., *Makromol. Chem.*, 1986, **187**, 1557.
18. Sterzynski, T. and Garbarczyk, J., *J. Mater. Sci.*, 1991, **26**, 6357.
19. Martuscelli, E., Canetti, M., Vicini, L. and Seves, A., *Polymer*, 1982, **23**, 331.
20. Bliznyuk, V. N., Shilov, V. V. and Lipatov, Yu. S., *J. Mater. Sci. Lett.*, 1985, **4**, 284.
21. Silvestre, C., Cimmino, S., Martuscelli, E., Karasz, E. and MacKnight, W. J., *Polymer*, 1987, **28**, 1190.
22. Cimmino, S., Di Pace, E., Martuscelli, E. and Silvestre, C., *Makromol. Chem.*, 1988, **9**, 261.
23. Ito, H., Russell, T. P. and Wignall, G. D., *Macromolecules*, 1987, **20**, 2213.
24. Hopkinson, I., Kiff, F. T., Richards, R. W., King, S. M. and Farren, T., *Polymer*, 1995, **36**, 3523.
25. Li, X. and Hsu, S. L., *J. Polym. Sci.*, 1984, **22**, 1331.
26. Ramana Rao, G., Castiglioni, C., Gussoni, M., Zerbi, G. and Martuscelli, E., *Polymer*, 1985, **26**, 811.
27. Makhija, S., Pearce, E. M. and Kwei, T. K., *J. Polym. Sci.: Part A: Polym. Chem.*, 1992, **30**, 2693.
28. Straka, J., Schmidt, P., Dybal, J., Schneider, B. and Spevacek, J., *Polymer*, 1995, **36**, 1147.
29. Shimada, S., Kashima, K., Hori, Y. and Kashiwabara, H., *Macromolecules*, 1990, **23**, 3769.
30. Miklesova, K. and Szocs, F., *Eur. Polym. J.*, 1992, **28**, 553.
31. Brosseau, C., Guillermo, A. and Cohen-Addad, J. P., *Polymer*, 1992, **33**, 2076.
32. Mansfield, P., *Phys. Rev.*, 1963, **137**, 961.
33. Jeener, J. and Broekaert, P., *Phys. Rev.*, 1967, **157**, 232.
34. Stejskal, E. O., Schaefer, J., Sefcik, M. D. and McKay, R. A., *Macromolecules*, 1981, **14**, 275.
35. Tékély, P., Nicole, D., Brondeau, J. and Delpuech, J. J., *J. Phys. Chem.*, 1986, **90**, 5608.
36. Tékély, P., Canet, D. and Delpuech, J. J., *Mol. Phys.*, 1989, **67**, 81.
37. Stejskal, E. O. and Schaefer, J., *J. Magn. Reson.*, 1975, **18**, 560.
38. Tegenfelt, J., Haeberlen, U. and Waugh, J. S., *J. Magn. Reson.*, 1979, **36**, 453.
39. Dechter, J. J., *J. Polym. Sci., Polym. Lett. Ed.*, 1985, **23**, 261.
40. Tékély, P., Lauprêtre, F. and Monnerie, L., *Polymer*, 1985, **26**, 1081.
41. Dickinson, L. C., Yang, H., Chu, C. W., Stein, R. S. and Chien, J. C. W., *Macromolecules*, 1987, **20**, 1757.